

Published in final edited form as:

Mol Cancer Ther. 2021 January 01; 20(1): 50–63. doi:10.1158/1535-7163.MCT-20-0480.

Repurposing the antidepressant sertraline as SHMT inhibitor to suppress serine/glycine synthesis addicted breast tumor growth

Shauni Lien Geeraerts^{1,2,†}, Kim Rosalie Kampen^{1,3,†}, Gianmarco Rinaldi^{4,5}, Purvi Gupta⁶, Mélanie Planque^{4,5}, Nikolaos Louros^{7,8}, Elien Heylen¹, Kaat De Cremer², Katrijn De Brucker², Stijn Vereecke¹, Benno Verbelen¹, Pieter Vermeersch⁹, Joost Schymkowitz^{7,8}, Frederic Rousseau^{7,8}, David Cassiman¹⁰, Sarah-Maria Fendt^{4,5}, Arnout Voet⁶, Bruno P.A. Cammue², Karin Thevissen^{2,‡,*}, Kim De Keersmaecker^{1,‡,*}

¹Laboratory for Disease Mechanisms in Cancer, Department of Oncology, KU Leuven and Leuven Cancer Institute (LKI), Herestraat 49, 3000 Leuven, Belgium ²Centre of Microbial and Plant Genetics – Plant Fungi Interactions (CMPG-PFI), KU Leuven, Kasteelpark Arenberg 20, 3001 Heverlee, Belgium ³Maastricht University Medical Center, Department of Radiation Oncology (MAASTRO), GROW School for Oncology and Developmental Biology, Maastricht, The Netherlands ⁴Laboratory of Cellular Metabolism and Metabolic Regulation, VIB-KU Leuven Center for Cancer Biology, VIB Leuven, Herestraat 49, 3000 Leuven, Belgium ⁵Laboratory of Cellular Metabolism and Metabolic Regulation, Department of Oncology, KU Leuven and Leuven Cancer Institute (LKI), Herestraat 49, 3000 Leuven, Belgium ⁶Department of Chemistry, KU Leuven, Celestijnenlaan 200G, 3001 Heverlee, Belgium ⁷Switch Laboratory, VIB Center for Brain and Disease Research, VIB-KU Leuven, Herestraat 49, 3000 Leuven, Belgium ⁸Switch Laboratory, Department of Cellular and Molecular Medicine, KU Leuven, Herestraat 49, 3000 Leuven, Belgium ⁹Department of Cardiovascular Sciences, University Hospitals Leuven, Herestraat 49, 3000 Leuven, Belgium ¹⁰Department of Hepatology, University Hospitals Leuven, Herestraat 49, 3000 Leuven, Belgium

Abstract

Metabolic rewiring is a hallmark of cancer that supports tumor growth, survival and chemotherapy resistance. While normal cells often rely on extracellular serine and glycine supply, a significant subset of cancers becomes addicted to intracellular serine/glycine synthesis, offering an attractive drug target. Previously developed inhibitors of serine/glycine synthesis enzymes did not reach clinical trials due to unfavorable pharmacokinetic profiles, implying that further efforts to identify clinically applicable drugs targeting this pathway are required. In this study, we aimed to develop therapies that can rapidly enter the clinical practice by focusing on drug repurposing, as their

* **Corresponding Authors:** Kim De Keersmaecker, KU Leuven, Laboratory for Disease Mechanisms in Cancer, Department of Oncology, KU Leuven and Leuven Cancer Institute (LKI), Campus Gasthuisberg O&N1, box 603, Herestraat 49, 3000 Leuven. Phone number: +32 16 37 31 67. kim.dekeersmaecker@kuleuven.be, Karin Thevissen, KU Leuven, Centre of Microbial and Plant Genetics – Plant Fungi Interactions (CMPG-PFI), Kasteelpark Arenberg 20, box 2460, 3001 Heverlee. Phone number: +32 16 32 96 88 or +32 16 32 16 31. karin.thevissen@kuleuven.be.

† Shared first authors

‡ Shared last authors

Disclosure of Potential Conflicts of Interest:

SMF has received funding from Bayer, Merck and Black Belt Therapeutics. All other authors declare no potential conflicts of interest.

safety and cost-effectiveness have been optimized before. Using a yeast model system, we repurposed two compounds, sertraline and thimerosal, for their selective toxicity against serine/glycine synthesis addicted breast cancer and T-cell acute lymphoblastic leukemia cell lines. Isotope tracer metabolomics, computational docking, enzymatic assays and drug-target interaction studies revealed that sertraline and thimerosal inhibit serine/glycine synthesis enzymes serine hydroxymethyltransferase and phosphoglycerate dehydrogenase, respectively. In addition, we demonstrated that sertraline's anti-proliferative activity was further aggravated by mitochondrial inhibitors, such as the antimalarial artemether, by causing G1-S cell cycle arrest. Most notably, this combination also resulted in serine-selective antitumor activity in breast cancer mouse xenografts. Collectively, this study provides molecular insights into the repurposed mode-of-action of the antidepressant sertraline and allows to delineate a hitherto unidentified group of cancers being particularly sensitive to treatment with sertraline. Furthermore, we highlight the simultaneous inhibition of serine/glycine synthesis and mitochondrial metabolism as a novel treatment strategy for serine/glycine synthesis addicted cancers.

Keywords

Breast cancer; Cancer metabolism; Serine/glycine synthesis; Sertraline; SHMT

Introduction

Rewiring of energy metabolism, exemplified by the Warburg effect, is one of the hallmarks of cancer (1). While normal cells often rely on serine/glycine uptake from their environment, several cancer subtypes produce their own serine/glycine via intracellular serine/glycine synthesis and become addicted to this own production (2,3). In general, serine/glycine synthesis (Fig. 1) consists of two processes: *de novo* serine synthesis from glucose and interconversion of serine into glycine. *De novo* serine synthesis branches from glycolysis, with the glycolytic intermediate 3-phosphoglycerate being converted into serine via three consecutive enzymatic reactions catalyzed by phosphoglycerate dehydrogenase (PHGDH), phosphoserine aminotransferase 1 (PSAT1) and phosphoserine phosphatase (PSPH). Thereafter, serine is catabolized into glycine, facilitated by serine hydroxymethyltransferase 1 or 2 (SHMT1/2), with 1 and 2 referring to the cell compartment in which the reaction takes place, i.e. the cytosol or the mitochondria (2,3). By relying on intracellular serine/glycine synthesis, cancer cells feed their high requirements to generate formate for purine synthesis, produce reductive equivalents to control redox homeostasis, regulate DNA demethylation and support lipid metabolism (3).

A cancer type well-known for its dependency on serine/glycine synthesis is breast cancer, where 6% of the patient samples display copy number gains of the *PHGDH* gene. Furthermore, 70% of estrogen receptor negative breast tumors have increased PHGDH protein levels, and inhibition of PHGDH via RNA interference or PHGDH inhibitors impairs cell proliferation and survival (4–8). Besides PHGDH, also SHMT2 is known to be exploited by breast cancer cells as SHMT2 expression levels are positively correlated with breast cancer grade (9). Additionally, *SHMT2* is identified as a direct target gene of the *MYC* oncogene (10). *MYC*-driven stimulation of *de novo* serine synthesis by transcriptional

upregulation of *PHGDH*, *PSAT1* and *PSPH* is also critical for sustaining survival and rapid proliferation of cancer cells under nutrient deprived conditions (11). Apart from *MYC*, the oncogene *KRAS*, the tumor suppressor p53, the mTOR-ATF4 axis and the T-cell leukemia associated R98S mutation in ribosomal protein L10 (RPL10 R98S) have also been shown to enhance serine/glycine synthesis in cancer cells (12–15).

Evidence for addiction to serine/glycine synthesis in cancer subsets, including triple-negative breast cancer and T-cell leukemia that are both currently treated with toxic intensive chemotherapy regimens, is growing. This highlights the necessity to develop novel therapeutic intervention strategies for these cancers, specifically focusing on targeting serine/glycine synthesis. *PHGDH* and *SHMT* inhibitors have been identified but did not enter clinical trials due to unfavorable pharmacokinetic profiles or because they have only recently been developed (7,8,16–18). Further efforts to identify clinically applicable drugs targeting this pathway are therefore required.

In this study, we made use of a lower eukaryotic yeast model system that specifically upregulates serine/glycine synthesis in response to sublethal stress. Using this platform, we discovered two repurposed compounds, sertraline and thimerosal (chemical structures in Fig. 5E) (19), that show selective toxicity to serine/glycine synthesis addicted cancer cell lines, while they had no effect on cancer and normal lymphoid cell lines that take up serine and glycine from their environment. Moreover, this work reports the potential application of the clinically used antidepressant sertraline as adjuvant therapeutic agent to treat serine/glycine synthesis addicted cancers, especially when combined with drugs causing mitochondrial dysfunction.

Materials And Methods

Cells

Breast cancer cell lines MDA-MB-231 (ATCC #HTB-26, RRID:CVCL_0062), MDA-MB-468 (ATCC #HTB-130, RRID:CVCL_0419), MCF7 (ATCC #HTB-22, RRID:CVCL_0031) and HCC70 (ATCC #CRL-2315, RRID:CVCL_1270) were cultured at 37°C and 5% CO₂ in DMEM (Gibco #41965039) supplemented with 10% fetal bovine serum (FBS; Gibco #10270-106). Because of many serial passages, MCF7 cell authenticity was confirmed by Microsynth AG. Other cell lines were freshly obtained from American Type Culture Collection (ATCC). The Ba/F3 pro-B cell line (DSMZ #ACC-300, RRID:CVCL_0161) was obtained from Leibniz-Institute DSMZ and grown in RPMI-1640 (Gibco #21875091) supplemented with 10% FBS and 10 ng/ml interleukin 3 (IL-3; Miltenyi). CRISPR-Cas9 engineering of Ba/F3 cells is described in the supplementary information. All cell lines were tested for *Mycoplasma* with the MycoAlert Mycoplasma Detection Kit (Lonza #LT07-418) before use and were cultured for maximum 49 days after thawing. Serine depleted media corresponds to DMEM without serine and glycine (US Biological Life Sciences #D9802-01), supplemented with 4.5 g/l glucose, 3.7 g/l sodium bicarbonate, 1:100 glutamax and 10% dialyzed serum (Gibco #A3382001).

Compounds

1000x stock solutions of each compound were made and stored at -20°C. Sertraline (Sigma-Aldrich #S6319), NCT-503 (Sigma-Aldrich #SML1659), rotenone (Sanbio #13995-100), antimycin A (Sigma-Aldrich #A8674) and artemether (TCI Europe #A2190) were dissolved in DMSO, while thimerosal (Sigma-Aldrich #T8784), benzalkonium chloride (Sigma-Aldrich #12060) and bupropion (TCI Europe #B3649) were dissolved in water. Sertraline's activity can differ between batches, causing variability in the exact dose that is required to obtain the observed effects.

Proliferation assay

MDA-MB-231 (7500 cells/well), MDA-MB-468 (7500 cells/well), MCF7 (4000 cells/well) and HCC70 (4500 cells/well) cells (100 µl) were seeded in 96-well plates (Sigma-Aldrich #Z707902-108EA) and incubated at 37°C for 24 hours to obtain optimal adherence to the surface. Next, 100 µl of 2x compound solutions, diluted in DMEM with 10% FBS, were added. During the following 5 days, cell proliferation was assessed by real-time imaging of confluency on an IncuCyte Zoom system (Essen BioScience). Using the exponential portions of the resulting growth curves, we calculated the growth rate (GR) under various drug conditions. The formula below was used, in which t1 and t2 are two time points within the exponential growth phase: $GR(1/h) = [\ln(\text{confluency } t2) - \ln(\text{confluency } t1)] / [\text{time}(t2) - \text{time}(t1)]$.

Ba/F3 viability assay

Three RPL10 WT versus three RPL10 R98S clones were plated and cultured for 72 hours to exhaust the medium. Afterwards, the clones were incubated with sertraline (7.3 µM) or thimerosal (1 µM). Relative cell viability was measured, using flow cytometry, after 48 hours of compound treatment.

Steady-state metabolite concentrations and ¹³C₆-glucose tracing

150.000 MDA-MB-468 cells were plated in 3 ml of DMEM in 6-well plates (VWR #734-0948). After 24 hours of incubation at 37°C, cells were washed with PBS and 3 ml of tracing medium (glucose-free DMEM with 10% dialyzed serum and 4.5 g/l ¹³C₆-glucose) was added. Subsequently, cells were incubated at 37°C during 24 hours (thimerosal and NCT-503) or 72 hours (sertraline and/or artemether). Metabolites for the subsequent mass spectrometry analysis were prepared by quenching the cells in liquid nitrogen followed by a cold two-phase methanol-water-chloroform extraction (20,21). Phase separation was achieved by centrifugation at 4°C (24x3.75 g, 10 minutes). The methanol-water phase containing polar metabolites was separated and dried using a vacuum concentrator at 4°C overnight. Dried metabolite samples were stored at -80°C. Polar metabolites were analyzed by GC-MS and LC-MS, as described in the supplementary information.

PHGDH *in vitro* enzymatic activity assay

PHGDH activity upon drug treatment was tested using human PHGDH (BPS Bioscience #71079) and a colorimetric PHGDH activity kit (BioVision #K569). PHGDH inhibitor NCT-503 served as a positive control (7). Human PHGDH was diluted in water to a

concentration of 0.15 mg/ml. Next, 5 μ l of this PHGDH enzyme solution and 10 μ l sertraline, thimerosal or NCT-503 was added in a 96-well plate (flat bottom). Subsequently, 35 μ l PHGDH assay buffer (BioVision #K569) and 50 μ l PHGDH reaction mix (prepared as described in #K569, BioVision) was added. Afterwards, absorbance at 450 nm was measured over time. In between measurements, the plate was incubated at 37°C, protected from light. Finally, PHGDH activity was calculated between two time points within the linear range of the internal standard (as described in #K569, BioVision).

Computational docking

Sertraline was modelled using MOE (Chemical Computing Group, Montreal, Canada) (MOE, RRID:SCR_014882) with the MMFF94x force field. The structures of the putative enzymes present in serine/glycine synthesis were obtained from the RCSB database (PDB ID SHMT1: 1BJ4, SHMT2: 5V7I). The bioactive conformations were chosen for each enzyme (SHMT1, SHMT2 as dimers) and optimized in MOE using protonate_3D. Docking was performed using GOLD8 software (22) (GOLD, RRID:SCR_000188). Specifically, sertraline was docked in the presence of the pyridoxal 5'-phosphate (PLP) co-factor. Furthermore, the known SHMT inhibitor (pyrazolopyran scaffold, SHIN1) and a library of FDA approved compounds (17,23) were docked in the presence of the PLP ligand. Conformational restraints were applied to the ligand by disallowing the flipping of ring conformations and planar R-NR1R2 groups to ensure the rigidity of sertraline. Each ligand was docked 10 times into each enzyme and the score was calculated using CHEMPLP scoring function. The interactions of sertraline with SHMT1/2 were analyzed and visualized using PyMOL version 1.8 (Schrödinger, 2015) (PyMOL, RRID:SCR_000305). The docked conformations of the ligands in SHMT1/2 were superimposed using PyMOL to compare the interactions. Ligand efficiency scores were calculated to normalize each docking score by the number of heavy atoms in each ligand.

Deuterated [2,3,3-²H]-serine tracing

150.000 MDA-MB-468 cells were plated in 2 ml of DMEM in 6-well plates (VWR #734-0948). After 24 hours of incubation at 37°C, cells were washed with PBS and 2 ml of serine-free DMEM (US Biological Life Sciences #D9802-01), supplemented with 4.5 g/l glucose, 3.7 g/l sodium bicarbonate, 400 μ M [2,3,3-²H]-serine, 400 μ M glycine, 1:100 glutamax and 10% dialyzed serum, was added for 48 hours. Metabolites for the subsequent mass spectrometry analysis were prepared by quenching the cells in liquid nitrogen followed by a cold two-phase methanol-water-chloroform extraction (20,21). Phase separation was achieved by centrifugation at 4°C (24x3.75 g, 10 minutes). The methanol-water phase containing polar metabolites was separated and dried using a vacuum concentrator at 4°C overnight. Dried metabolite samples were stored at -80°C. Polar metabolites were analyzed by GC-MS and LC-MS, as described in the supplementary information.

Protein thermal shift

Recombinant human SHMT1 (Novusbio #NBPI-72548) was diluted in buffer (20 mM Tris-HCl pH 8.0 and 100 mM NaCl) to a concentration of 5 μ M. Thermal scanning was performed in clear 96-well PCR plates with in each well 4 μ M SHMT1, 5x SYPRO Orange (Invitrogen #S6650; 5000x) and 1.5 μ l sertraline (7 mM stock in 50% DMSO) in a total

volume of 15 μ l. In each well, the DMSO background was normalized to 5%. Dual SHMT1/2 inhibitor SHIN1, at a concentration of 250 μ M, served as a positive control (17). Unfolding was monitored by real-time PCR (CFX Connect, Bio-Rad Laboratories) and fluorescence intensity was measured every 20 seconds in the FRET channel over a linear 20°C to 95°C gradient of 1.5°C/min. Plots of the first derivative of fluorescence versus temperature were generated in CFX software.

Microscale thermophoresis (MST)

Recombinant human SHMT2 (OriGene #TP760127) was fluorescently labeled using the Monolith NT protein labeling kit Red-NHS (NanoTemper Technologies). For MST, the SHMT2 enzyme concentration was kept constant at 50 nM, whereas sertraline was titrated down from 730 μ M to 0.36 μ M. The DMSO background was kept constant at 5% and dual SHMT1/2 inhibitor SHIN1 (500 μ M) served as a positive control (17). The MST buffer contained 25 mM Tris-HCl pH 8.0, 150 mM NaCl, 0.5% glycerol and 0.05% sarkosyl for determining sertraline's binding affinity to SHMT2. MST with SHIN1 was performed in 25 mM Tris-HCl pH 8.0, 150 mM NaCl, 0.1% glycerol and 0.01% sarkosyl. Measurements were performed using Monolith NT automated premium capillaries and recorded on a Monolith NT automated instrument (NanoTemper Technologies) with a pico-red laser channel at 7% excitation power and "medium" MST power. The affinity constant (K_d) and experimental data fitting was performed using MO.Affinity analysis software. The thermophoretic movement of bound and unbound state superposed linearly. Therefore, the fraction bound (f) is described as $F_{\text{norm}} = (1-f) F_{\text{norm,unbound}} + (f) F_{\text{norm,bound}}$, where F_{norm} is the normalized fluorescence, $F_{\text{norm,unbound}}$ corresponds to the normalized fluorescence of the unbound state and $F_{\text{norm,bound}}$ is the normalized fluorescence of the bound state.

Uptake and secretion rates

150.000 MDA-MB-468 cells were plated in 2 ml of DMEM in 6-well plates (VWR #734-0948). The day after (day 0), cells were washed with PBS and 2 ml of fresh DMEM was added. 72 hours later (day 3), medium samples were taken (0.5-1 ml). The cells were counted on day 0 and on day 3, using an automated cell counter. Medium samples were analyzed by GC-MS, as described in the supplementary information. Specifically, uptake and secretion rates were calculated by subtracting metabolite concentrations of treated samples from those of culture media incubated for the same amount of time but without cells. Finally, results were normalized for both cell number and growth rate.

Cell death analysis

Cell death was quantified using a combined Zombie Aqua – eFluor506 and Annexin V – PE staining. 150.000 MDA-MB-468 cells were plated in 2 ml of DMEM in 6-well plates (VWR #734-0948) and incubated at 37°C for 24 hours to obtain optimal adherence to the surface. The day after, cells were treated with 2 ml of fresh DMEM containing sertraline (5, 7.5 or 10 μ M) and/or artemether (80 μ M). Upon 24 hours of treatment, cells were collected in a 96-well U-bottom plate and washed with PBS. Afterwards, cell viability was analyzed following incubation with Zombie Aqua (BioLegend #423102, 1:1000 in PBS) for 20 minutes at RT in the dark, an Annexin V binding buffer (Invitrogen #V13246) washing step and Annexin V (IQ Products #IQP-120R, 1:100 in binding buffer) staining at RT in the dark

for 15 minutes. All samples were acquired using a FACS Canto II flow cytometer and analyzed with FlowJo V10 (FlowJo, RRID:SCR_008520).

Cell cycle analysis

Cell cycle was analyzed by bromodeoxyuridine (BrdU) incorporation and propidium iodide (PI) staining. 150,000 MDA-MB-468 cells were plated in 2 ml of DMEM in 6-well plates (VWR #734-0948) and incubated at 37°C for 24 hours to obtain optimal adherence to the surface. The day after, cells were treated with 2 ml of fresh DMEM containing sertraline (5, 7.5 or 10 µM) and/or artemether (80 µM). Upon 24 hours of treatment, cells were incubated with 10 µM BrdU (eBioscience #00-4440-51A) at 37°C for 1 hour. Next, cells were collected using trypsin and washed with PBS. Afterwards, BrdU incorporation and PI staining were analyzed following 70% ice-cold ethanol fixation, 2 M HCl denaturation, 0.5 M EDTA (pH 8.0) neutralization, BrdU-FITC antibody (BioLegend #364104, RRID:AB_2564481) staining for 20 minutes at RT and 20 minutes incubation with PI solution (100 µg/ml) at RT. All samples were acquired using a FACS Canto II flow cytometer and analyzed with FlowJo V10 (FlowJo, RRID:SCR_008520).

Xenografts in NOD-SCID/IL2γ^{-/-} (NSG) mice

Animal experiments were approved by the local ethics committee (P262-2015). 3x10⁶ breast cancer cells were injected subcutaneously in the left (MDA-MB-231) and right (MDA-MB-468) flanks in a 1:1 mixture with matrigel (Corning). The mice (IMSR #JAX:005557, RRID:IMSR_JAX:005557) were monitored on a daily basis and sacrificed after 28 days. Mice received treatments on days 7, 9, 11, 13, 15, 20 and 24. Therapy was administered via intra-peritoneal injections at dosages of 2.5 mg/kg sertraline and/or 40 mg/kg artemether. Control mice were treated with DMSO.

Statistics

All statistical analyses were performed using GraphPad Prism 8 software (GraphPad Prism, RRID:SCR_002798) and data are presented as mean ± standard deviation (SD). Specific statistical tests used for each experiment are mentioned in the figure legends. Results were considered to be statistically significant if the adjusted p-value was < 0.05 (*p < 0.05, **p < 0.01, ***p < 0.001, ****p < 0.0001).

Results

Identification of selective inhibitors of serine/glycine synthesis addicted breast cancer cell lines

To address the need for clinically applicable drugs targeting serine/glycine synthesis, we focused on drug repurposing with the aim to develop novel therapies that can rapidly enter the clinical practice as their safety and pharmacokinetics have been validated in patients before. To do this, we made use of the lower eukaryotic yeast *Candida albicans* that specifically upregulates serine/glycine synthesis as a tolerance mechanism against sublethal stress (Supplementary Fig. S1A-B) (24,25), and hypothesized that compounds re-sensitizing this yeast to the antifungal stress, can be potent inhibitors of serine/glycine synthesis. Subsequently, “re-sensitizing hits” were further validated in a cancer context, both *in vitro*

and *in vivo*, by investigating their selective anti-proliferative effects on serine/glycine synthesis addicted cancer cell lines and delineating their exact mode-of-action (Fig. 1). Interestingly, the serotonin reuptake inhibitor sertraline was identified as a re-sensitizing agent, implying that it might stem from inhibition of serine/glycine synthesis (Supplementary Fig. S1C). This drug caught our attention, as sertraline is widely used in the clinic as antidepressant of which its safety for chronic use is well-documented.

To investigate whether sertraline is a specific inhibitor of serine/glycine synthesis, we tested its efficacy on cancer cell lines representing two subtypes of breast cancer, being those that rely on serine/glycine synthesis (MDA-MB-468) and those that depend on serine/glycine uptake (MDA-MB-231) (6,26). MDA-MB-468 cells typically express higher transcript and protein levels of serine/glycine synthesis enzymes (6,26), and flux through this metabolic pathway is associated with proliferation and sustained survival (6). We performed $^{13}\text{C}_6$ -glucose tracing to monitor the activity of serine/glycine synthesis in these cell lines. In such experiments, synthesis of serine and glycine can be monitored by following carbon-13 stable isotope incorporation from glucose, with glucose-derived serine and glycine showing mass shifts of 3 and 2 units (M+3 serine and M+2 glycine), respectively. Cellular uptake of unlabeled serine and glycine from the cell culture medium will, on the other hand, result in unlabeled (M+0) serine and glycine, whereas interconversion between serine and glycine, catalyzed by SHMT1/2, will result in partially labeled serine (M+1 and M+2) and glycine (M+1) (Fig. 3D). Our data confirmed that MDA-MB-468 cells showed around 10% serine M+3 and glycine M+2 contribution from labeled glucose, while serine and glycine were unlabeled in MDA-MB-231 cells (Supplementary Fig. S2A). MDA-MB-468 cells are thus able to endogenously produce serine and glycine, whereas MDA-MB-231 cells are not. In agreement with this, real-time monitoring of cell confluency of both cell lines treated with NCT-503, an established PHGDH inhibitor (7), showed dose-dependent inhibition of MDA-MB-468 proliferation, while minimal effects on MDA-MB-231 were observed (Supplementary Fig. S2B-C). Accordingly, treatment of MDA-MB-468 cells with sertraline induced a dose-dependent impairment of cell proliferation, whereas MDA-MB-231 cells were hardly affected (Fig. 2; Supplementary Fig. S3). These results indicate that compounds re-sensitizing the yeast model system, can specifically inhibit the proliferation of serine/glycine synthesis addicted breast cancer cells.

Besides sertraline, a previously performed screening of 1600 off-patent drugs and other bioactive compounds (Pharmakon 1600 repurposing library) using the same yeast model system as described above, resulted in the identification of 49 other “re-sensitizing hits” (Supplementary Table S1) (24,27). We hypothesized that this list might include other potent serine/glycine synthesis inhibitors (25). To select additional candidates for validation in serine/glycine synthesis addicted breast cancer cell lines, all 49 agents were ranked into three classes based on their yeast re-sensitizing capacity (high, intermediate and low). One representative agent of each class was retained for further validation, taking into account their clinical usage, as well as the presence of sulfhydryl containing groups that are proven to be effective for inhibition of PHGDH enzyme activity (8). Quaternary ammonium compounds came out as the top “hits” in the highest ranked class, of which we selected benzalkonium chloride. Out of the intermediate class of re-sensitizing agents, we selected thimerosal due to the presence of a reactive sulfhydryl group in its chemical structure.

Bupropion, representing the lowest ranked class, was also retained for testing since it is clinically used as antidepressant, similar to sertraline. Thimerosal and benzalkonium chloride showed selective inhibitory activity against serine/glycine synthesis addicted MDA-MB-468 cells (Fig. 2; Supplementary Fig. S3). Conversely, bupropion did not show any anticancer activity, not even at high concentrations (Fig. 2; Supplementary Fig. S3).

To validate these results, we selected a second pair of breast cancer cell lines, of which one is dependent on serine/glycine synthesis (HCC70) and one favors serine/glycine uptake from the microenvironment (MCF7) (6,26). As expected, PHGDH inhibitor NCT-503 induced a stronger inhibition of proliferation in HCC70 than in MCF7, especially at lower drug doses (Supplementary Fig. S4A-B). In agreement with previous results, sertraline, thimerosal and benzalkonium chloride impaired HCC70 cell proliferation in a dose-dependent manner, while there was no or minor toxicity on MCF7 cells (Supplementary Fig. S5A-B). Overall, thimerosal showed the highest selectivity in targeting serine/glycine synthesis addicted breast cancer cells as compared to sertraline and benzalkonium chloride, while sertraline, as an antidepressant, has highest potential for clinical use in cancer patients. We therefore selected both compounds for further characterization of their mode-of-action.

Sertraline and thimerosal target serine/glycine synthesis

Next, we verified whether sertraline and thimerosal would be applicable as agents that target serine/glycine synthesis addicted cancers other than breast cancer. The ribosomal RPL10 R98S mutation is detected in 8% of pediatric T-cell acute leukemia patients (28). In leukemic cells carrying this mutation, the mutant ribosomes accumulate on PSPH mRNAs, leading to elevated PSPH protein translation associated with enhanced serine/glycine synthesis. We showed that RPL10 R98S leukemic cancer cells depend on this elevated PSPH expression to support their proliferation and *in vivo* expansion (14). As such, RPL10 R98S leukemias represent a second cancer subgroup that is addicted to intracellular serine/glycine synthesis and we hypothesized that RPL10 R98S mutant cells might be more sensitive to sertraline and thimerosal. We used mouse pro-B Ba/F3 cells in which the endogenous Rpl10 locus was engineered with CRISPR/Cas9 technology to express the WT or R98S mutant form of RPL10, comparing three independent single cell clones of each genotype. RPL10 R98S clones showed selective inhibition of cell survival upon sertraline or thimerosal treatment as compared to the RPL10 WT clones (Fig. 3A). These results confirm applicability of sertraline and thimerosal in serine/glycine synthesis addicted cancer types other than breast cancer and suggest that these agents may target different serine/glycine synthesis addicted cancer subtypes.

To define the mode-of-action of both compounds, we first evaluated whether serine depletion from the culture medium increases the sensitivity of MDA-MB-468 breast cancer cells to sertraline and thimerosal by enforced dependency on intracellular serine/glycine synthesis. Only sertraline induced a significantly stronger impairment of MDA-MB-468 cell proliferation under serine-depleted conditions (Fig. 3B; Supplementary Fig. S6A-B). A similar trend was observed with NCT-503 (Supplementary Fig. S6C-D).

Given that MDA-MB-468 cells rely more on synthesis than uptake, inhibition of serine/glycine synthesis could cause changes in intracellular serine/glycine abundance, depending

on the specific synthesis enzyme that is targeted. While reductions in enzymatic activity of PHGDH, PSAT1 or PSPH are expected to result in reduced intracellular concentrations of both serine and glycine, targeting SHMT1/2 is rather expected to affect levels of glycine only. Mass spectrometry analysis revealed that sertraline did not affect the intracellular levels of serine in MDA-MB-468 cells, and that it solely reduced the abundance of downstream glycine (Fig. 3C). In contrast, thimerosal decreased serine abundance to the same extent as glycine, as seen for NCT-503 (Fig. 3C; Supplementary Fig. S6E).

We subsequently performed $^{13}\text{C}_6$ -glucose tracing to monitor the effects of sertraline and thimerosal on overall serine/glycine synthesis in more detail (Fig. 3D). Our data showed that sertraline reduced *de novo* synthesized M+3 serine, and that it targets serine to glycine interconversion in MDA-MB-468 cells, characterized by a reduced fractional labeling of M+2 glycine and M+1 serine (Fig. 3E). In contrast to sertraline, thimerosal did not significantly reduce the fraction of glucose-derived M+3 serine and M+2 glycine (Fig. 3E). In parallel, NCT-503 only caused minor changes in fractional glucose contribution of M+3 serine and M+2 glycine that could not solely account for the lower intracellular serine and glycine abundances (Supplementary Fig. S6E-F). Since we assess with this tracing the ratio between synthesis and uptake, our data may indicate a simultaneous downregulation of serine/glycine synthesis and uptake upon thimerosal or NCT-503 treatment.

Collectively, we reasoned that thimerosal, similar to NCT-503, is more likely to affect one of the three first biosynthetic enzymes. For sertraline, our data point towards inhibition of serine to glycine interconversion, implying that SHMT1/2 can be its potential target. In line with this hypothesis, steady state levels of serine (Fig. 3C) may originate from a block in conversion to glycine and subsequent downregulation of *de novo* serine synthesis and uptake.

Thimerosal reduces PHGDH activity, while sertraline inhibits SHMT1/2

To gain additional insights in the exact serine/glycine synthesis enzyme targeted by sertraline and thimerosal, we first performed an *in vitro* enzymatic PHGDH assay. Sertraline did not show any effect on PHGDH activity, further excluding PHGDH as sertraline's potential target (Fig. 4A). Similar to NCT-503, thimerosal was able to reduce PHGDH activity (Fig. 4A). Notably, the thimerosal concentration inducing 50% inhibition ($\text{IC}_{50} = 0.1517 \mu\text{M}$) was even 10-fold lower than this of NCT-503 ($\text{IC}_{50} = 1.747 \mu\text{M}$) (Fig. 4A; Supplementary Fig. S7A).

Since our *in vitro* enzymatic PHGDH assay had excluded PHGDH as sertraline's target and previous data already pointed towards more downstream inhibition of serine/glycine synthesis (Fig. 3), we focused further on SHMT1/2. First, we computationally docked sertraline to SHMT1 and SHMT2. It has been shown that SHMT is a ubiquitous pyridoxal 5'-phosphate (PLP)-dependent enzyme (17,29). Therefore, docking scores were determined with the PLP co-factor inside the binding pocket (Table 1). As a reference, the already reported plant derived and non-clinically used dual SHMT1/2 inhibitor with a pyrazolopyran scaffold, SHIN1, was used (17,30). High docking scores were obtained for sertraline, in the range of the compounds characterized by a pyrazolopyran scaffold. Moreover, aligning both

dockings showed that sertraline potentially binds in the exact same pocket as SHIN1 and has similar interactions with SHMT1/2, namely a hydrogen bond with its -NH group (Fig. 4B).

Next, a virtual library screen was performed by docking a library of 6392 FDA-approved ligands to SHMT1/2 (23). We observed that sertraline scores are average for both SHMT1 and SHMT2 (Supplementary Fig. S7B). Because sertraline is a very small molecule with only one option to create a high scoring hydrogen bond, the scoring function will assign a lower docking score to sertraline as compared to larger molecules with more hydrophilic groups. We therefore calculated the ligand efficiency score, which adds a normalization for the amount of heavy atoms in each ligand to the docking score. This significantly improved the prediction for sertraline binding to SHMT1/2 and even assigned a higher score to sertraline as compared to the clinically used SHMT inhibiting antifolates pemetrexed and lometrexol (Supplementary Fig. S7B and Table S2-3).

To experimentally measure cellular SHMT activity upon sertraline treatment, we performed isotopic hydrogen tracing (Fig. 4C) in which MDA-MB-468 cells were incubated with [2,3,3-²H]-serine, followed by analysis of ²H incorporation in glycine and thymidine triphosphate (dTTP) (31). These tracings revealed that sertraline increased the intracellular fraction of M+3 serine and decreased the fraction of M+0, M+1 and M+2 serine (Fig. 4D). While M+3 serine is used by SHMT1/2 to convert to glycine, partially labelled serine (M+1 and M+2) only arises from converting glycine back into serine. Furthermore, only M+1 dTTP was detected in MDA-MB-468 (Supplementary Fig. S7C), supporting that these cells process their 1C units only in the mitochondria via SHMT2 (31,32). Interestingly, the M+1 dTTP fraction was decreased upon sertraline treatment (Fig. 4E). Accordingly, binding of sertraline to SHMT2 was confirmed by microscale thermophoresis ($K_d = 13.1 \mu\text{M}$) (Fig. 4F), using SHIN1 as a positive control (Supplementary Fig. S7D) (17). In addition, sertraline decreased the melting temperature of SHMT1 as measured by a thermal shift assay (Fig. 4G), consistent with decreased stability of SHMT1 upon binding of SHIN1 (Supplementary Fig. S7E). These findings identify sertraline as dual SHMT1/2 inhibitor.

In contrast to what may be expected from an SHMT inhibitor, sertraline did not increase the intracellular serine levels (Fig. 3C). To look closer into this, we determined the impact of sertraline on serine/glycine uptake and secretion rates in MDA-MB-468 cells (Fig. 4H). Our data showed a dose-dependent reduction of net serine uptake. Upon the highest sertraline dose, we even observed net serine secretion. These observations can explain the lack of serine accumulation in these breast cancer cells. Whether these effects are due to direct serine secretion and/or a sensory feedback mechanism of pyruvate kinase (PKM2), an important regulator of the glycolytic flux, remains to be determined. Furthermore, measuring glycine uptake and secretion rates revealed that sertraline-treated MDA-MB-468 cells have the tendency to take up less glycine (Fig. 4H). The strength of blocking both the serine into glycine interconversion and glycine uptake is what makes SHMT inhibitors more cytotoxic, explaining sertraline's potent activity on MDA-MB-468 cells, as was previously also observed using SHIN1 (17). Together, these results support that sertraline inhibits SHMT1/2 activity and glycine uptake, leading to reduced net serine uptake and *de novo* serine synthesis, to prevent serine accumulation.

Sertraline has clinical potential in combination therapy

In contrast to thimerosal, for which clinical applications are limited to topical use because of a toxic mercury group in its structure, sertraline is a small molecule antidepressant. Our findings support that sertraline can be an attractive adjuvant therapeutic agent to specifically treat serine/glycine synthesis addicted cancers.

It has been established that mitochondrial dysfunction causes changes in one-carbon metabolism and that cancer cells will depend even more on serine/glycine synthesis upon mitochondrial inhibition (33,34). Furthermore, serine/glycine synthesis and the tricarboxylic acid (TCA) cycle are strongly interconnected, implying that targeting both serine/glycine synthesis and mitochondrial metabolism might further metabolically disrupt cancer cells. As a proof-of-concept, we investigated the effect of sertraline on MDA-MB-468 proliferation when combined with suboptimal dosages of mitochondrial inhibitors rotenone and antimycin A, targeting respiratory chain complex I and III, respectively (35). While sertraline monotherapy caused around 20% reduction in cell proliferation, combining sertraline with rotenone or antimycin A further decreased proliferation of MDA-MB-468. No synergistic effect of both combinations on MDA-MB-231 proliferation was observed (Fig. 5A; Supplementary Fig. S8A-C).

To further analyze sertraline's clinical potential in combination therapy, we tested sertraline in combination with a clinically used and less generally toxic drug than rotenone and antimycin A. Artemether, an antimalarial agent, has already been shown to have potent anticancer activity (36,37). Interestingly, artemisinin, which belongs to the same structural class as artemether, was identified as activator of AMPK, suggesting a possible inhibition of mitochondrial function (38). By performing $^{13}\text{C}_6$ -glucose tracing of artemether-treated MDA-MB-468 cells (Supplementary Fig. S9), we confirmed inhibitory action of artemether on mitochondrial TCA cycle activity, as evidenced by decreased contribution of labeled glucose into TCA cycle metabolites, especially the M+4 variants. Besides, a slight reduction of the M+3 serine fraction was detected, but this was lower than the observed inhibitory effect on TCA cycle intermediates. Additionally, glucose contribution into M+3 lactate and M+3 alanine was elevated upon artemether treatment, which was not observed with sertraline. The latter suggests that overall TCA cycle activity is reduced, and pyruvate will use alternative routes such as its reduction to lactate, supporting that artemether acts as mild mitochondrial inhibitor. Corresponding to what was observed using the well-established mitochondrial inhibitors rotenone and antimycin A, the artemether-sertraline combination indeed further decreased MDA-MB-468 cell proliferation as compared to single drug treatment, while minimal effects were observed on MDA-MB-231 cells (Fig. 5A; Supplementary Fig. S8B-C). $^{13}\text{C}_6$ -glucose tracing confirmed the superior effect of this novel combination therapy as the contribution of labeled glucose into TCA cycle metabolites was stronger reduced (Supplementary Fig. S9). In contrast, the reduction in M+3 serine and M+2 glycine was identical to this of sertraline monotherapy, confirming that the inhibitory effect on serine/glycine synthesis is rather due to sertraline than to artemether.

Since the artemether-sertraline combination mainly reduced the MDA-MB-468 proliferation rate, we hypothesized that it interferes with cell cycle progression rather than inducing cell death. Indeed, bromodeoxyuridine (BrdU) staining showed a significant decrease in BrdU

incorporation in MDA-MB-468 cells upon combination treatment, compared to monotherapy (Fig. 5B-C; Supplementary Fig. S10B). Moreover, propidium iodide (PI) cell cycle analysis confirmed a G1-S cell cycle arrest, with 20% more MDA-MB-468 cells in G1-phase upon combination treatment (Fig. 5B-C; Supplementary Fig. S10B). Only 5% of MDA-MB-468 cells were double positive for the Annexin V and Zombie Aqua cell death markers after combination treatment (Supplementary Fig. S10C), supporting limited effects on cell apoptosis. Apart from the artemether-sertraline combination, minor effects on cell cycle were observed with a suboptimal dose of sertraline that increases with increased doses of sertraline (Supplementary Fig. S10A-B). As such, artemether strengthens sertraline's inhibitory effect on G1-S cell cycle progression, highlighting the potential of a mitochondrial inhibitor in combination with sertraline.

To evaluate the therapeutic potential of these findings more profoundly, we tested the efficacy of the artemether-sertraline combination in an *in vivo* mouse model. To this end, we implanted MDA-MB-231 and MDA-MB-468 cells in the opposite flanks of immunodeficient NOD-SCID/IL2 γ ^{-/-} (NSG) mice and treated the animals with sertraline (2.5 mg/kg), artemether (40 mg/kg) or a combination of both. After 4 weeks, only the MDA-MB-468 mouse xenografted tumors showed significant differences between treatment groups and artemether significantly reduced MDA-MB-468 tumor growth (Fig. 5D). Most notably, the artemether-sertraline combination caused an even stronger inhibition of MDA-MB-468 tumor formation as compared to monotherapy (Fig. 5D). No changes in MDA-MB-231 tumor growth were observed between treatment groups within the same mice (Fig. 5D). Collectively, this highlights the potency of a mitochondrial inhibitor, such as artemether, in combination with sertraline to treat serine/glycine addicted cancers.

Discussion

Our data support upregulation of serine/glycine synthesis as a general mechanism to deal with cellular stress that has been evolutionary conserved from the lower eukaryote *Candida albicans* up to human cancer cells. Hence, this yeast model system can be used for rapid and low-cost screening for compounds targeting serine/glycine synthesis. Further characterization of the mode-of-action of “re-sensitizing hits” revealed that sertraline and thimerosal target intracellular serine/glycine synthesis enzymes SHMT1/2 and PHGDH, respectively (Fig. 5E).

Although thimerosal showed potent PHGDH inhibition with 10-fold lower IC₅₀ values compared to NCT-503, its clinical applications are limited to topical use due to the presence of a toxic mercury group in its chemical structure. Therefore, we tested thimerosal derivatives that do not contain a mercury group (methyl thiosalicylate, thiosalicylic acid and sodium thiosalicylate) for their potential to inhibit MDA-MB-468 proliferation. However, these compounds did not affect MDA-MB-468 proliferation, nor could they inhibit *in vitro* PHGDH enzymatic activity. In agreement with these observations, it was previously described that thimerosal's sulfhydryl reactive properties, which are expected to be important for inhibiting PHGDH activity, are attributable to its mercury-containing chemical structure (8,39). In line with an important role for sulfhydryl reactive properties in inhibiting PHGDH, compound CBR-9480, being very similar in chemical structure with thimerosal,

was also picked up as a potent PHGDH inhibitor (8). As opposed to thimerosal, the antidepressant sertraline has high clinical potential as targeting agent for serine/glycine synthesis addicted cancers.

Besides T-cell leukemia (14,16) and breast cancer, upregulation of serine/glycine synthesis is also known in other cancer types such as melanoma, glioblastoma, prostate, testis, ovary, liver, kidney, lung and pancreas cancer (40,41). Expression levels of serine/glycine synthesis enzymes reaching above 4-fold increased expression as compared to normal tissue controls (based on our Ba/F3 RPL10 WT and R98S model), may serve as a biomarker to identify serine/glycine synthesis addicted cancers that may benefit from sertraline treatment.

Whereas antitumor activity of sertraline has previously been described (42–44), our findings pinpoint the exact mode-of-action of its anticancer activity and support that this agent could also be an attractive adjuvant therapeutic agent to specifically treat the subset of serine/glycine synthesis addicted cancers. Moreover, suppression of serine/glycine synthesis has been shown to re-sensitize therapy resistant tumors to anticancer treatment. In particular, PHGDH targeting resulted in re-sensitization to doxorubicin, vemurafenib and HIF2 α -antagonist in therapy resistant triple-negative breast cancer cells, melanoma with oncogenic BRAF V600E mutations and advanced renal cell carcinoma, respectively (45–47). Additionally, sertraline passes the blood-brain barrier, which may even open opportunities to target serine/glycine synthesis addicted brain tumors.

The doses at which we observed activity against serine/glycine synthesis addicted cancer cell lines are in the range of concentrations at which sertraline's antitumor activity was described by others (42–44). Clinical use of sertraline as adjuvant anticancer therapy will only be possible if the dosages required for anticancer efficacy are not reaching toxicity in humans. As an antidepressant, sertraline is administered in a dosage ranging from 50 to 200 mg/day, resulting in serum concentrations between 0.065 and 0.54 μ M (48). Considering that the average body weight of an adult in Europe is 70.8 kg (49), sertraline doses vary between 0.7 and 2.8 mg/kg. Furthermore, sertraline has a linear pharmacokinetic profile and daily oral intake of 400 mg (5.6 mg/kg) is well tolerated in patients (43,48). In our *in vivo* experiments, we treated the mice with 2.5 mg/kg sertraline, which thus is in the range of the administered doses in humans. Hassell *et al.* even used 60 mg/kg sertraline in mice and no adverse effects were observed (43). This suggests that therapeutic doses of sertraline can be achieved in cancer patients.

Serine/glycine uptake dependent cancers can become addicted to serine/glycine synthesis upon serine-starvation (50). However, metabolic adaptation of synthesis addicted cancer cells by re-uptake of serine/glycine from their environment under long-term SHMT or PHGDH inhibition has not been reported yet. Such a potential resistance mechanism again underscores the importance of using a combination therapy as we propose.

In conclusion, we identified the widely used antidepressant sertraline as a novel inhibitor of serine/glycine synthesis enzyme SHMT that demonstrated high efficacy against metabolically addicted cancers. Whereas previously identified inhibitors of serine/glycine synthesis enzymes did not reach clinical trials, sertraline is a clinically used drug that can

safely be used in humans. Our results suggest that sertraline may have applications as adjuvant therapeutic intervention strategy for serine/glycine synthesis addicted cancers, especially when combined with drugs attacking other central nodes of cancer cell metabolism such as mitochondrial inhibitors. Collectively, this work provides a novel and cost-efficient treatment option for the rapidly growing list of serine/glycine synthesis addicted cancers.

Supplementary Material

Refer to Web version on PubMed Central for supplementary material.

Acknowledgments

We thank Annelies Peeters and Tamara Davenne for technical support. SL Geeraerts received a SB PhD fellowship from “Fonds Wetenschappelijk Onderzoek (FWO)” (1S14517N). KR Kampen was supported by a PDM postdoctoral mandate fellowship obtained from the KU Leuven, the “Emmanuel van der Schueren” postdoctoral fellowship from “Kom op tegen Kanker” and a research grant from FWO (FWO KAN2018 1501419N). G Rinaldi is supported by consecutive PhD fellowships from the “Emmanuel van der Schueren - Kom op tegen Kanker” foundation and FWO (1137117N and 1137119N). P Gupta and A Voet acknowledge a research grant from FWO (G0F9316N Odysseus). The Switch Laboratory was supported by grants from the European Research Council under the European Union’s Horizon 2020 Framework Programme ERC Grant Agreement (647458 (MANGO) to JS); the Flanders Institute for Biotechnology (VIB; grant no. C0401); the Industrial Research Fund of KU Leuven (“Industrieel Onderzoeksfonds (IOF)”); the Funds for Scientific Research Flanders (FWO; Hercules Foundation grant AKUL/15/34 - G0H1716N); the Flanders Agency for Innovation by Science and Technology (IWT; SBO grant 60839). N Louros was funded by Fund for Scientific Research Flanders Post-doctoral fellowship (FWO 12P0919N). E Heylen received a FWO PhD fellowship fundamental research (1106121N). S Vereecke and B Verbelen are SB PhD fellow at FWO (1S07118N and 1S49817N). P Vermeersch and D Cassiman are senior clinical investigators of the Research Foundation - Flanders. SM Fendt acknowledges FWO funding and KU Leuven Methusalem co-funding. K Thevissen received a mandate as Innovation Manager from IOF Fund of KU Leuven. This research was funded by a grant from “Stichting Tegen Kanker” (2016-112) and by funding from the KU Leuven Research Council (C1 grant C14/18/104) to K De Keersmaecker.

References

- Hanahan D, Weinberg RA. Hallmarks of Cancer: The Next Generation. *Cell*. 2011; 144:646–74. [PubMed: 21376230]
- Locasale JW. Serine, glycine and one-carbon units: cancer metabolism in full circle. *Nat Rev Cancer*. 2013; 13:572–83. [PubMed: 23822983]
- Amelio I, Cutruzzolá F, Antonov A, Agostini M, Melino G. Serine and glycine metabolism in cancer. *Trends Biochem Sci*. 2014; 39:191–8. [PubMed: 24657017]
- DeBerardinis RJ. Serine Metabolism: Some Tumors Take the Road Less Traveled. *Cell Metab*. 2011; 14:285–6. [PubMed: 21907134]
- Locasale JW, Grassian AR, Melman T, Lyssiotis CA, Mattaini KR, Bass AJ, et al. Phosphoglycerate dehydrogenase diverts glycolytic flux and contributes to oncogenesis. *Nat Genet*. 2011; 43:869–74. [PubMed: 21804546]
- Possemato R, Marks KM, Shaul YD, Pacold ME, Kim D, Birsoy K, et al. Functional genomics reveal that the serine synthesis pathway is essential in breast cancer. *Nature*. 2011; 476:346–50. [PubMed: 21760589]
- Pacold ME, Brimacombe KR, Chan SH, Rohde JM, Lewis CA, Swier LJYM, et al. A PHGDH inhibitor reveals coordination of serine synthesis and one-carbon unit fate. *Nat Chem Biol*. 2016; 12:452–8. [PubMed: 27110680]
- Mullarky E, Lucki NC, Beheshti Zavareh R, Anglin JL, Gomes AP, Nicolay BN, et al. Identification of a small molecule inhibitor of 3-phosphoglycerate dehydrogenase to target serine biosynthesis in cancers. *Proc Natl Acad Sci*. 2016; 113:1778–83. [PubMed: 26831078]

9. Yin K. Positive correlation between expression level of mitochondrial serine hydroxymethyltransferase and breast cancer grade. *Onco Targets Ther.* 2015; 8:1069–74. [PubMed: 25999742]
10. Nikiforov MA, Chandriani S, O’Connell B, Petrenko O, Kottenko I, Beavis A, et al. A functional screen for Myc-responsive genes reveals serine hydroxymethyltransferase, a major source of the one-carbon unit for cell metabolism. *Mol Cell Biol.* 2002; 22:5793–800. [PubMed: 12138190]
11. Sun L, Song L, Wan Q, Wu G, Li X, Wang Y, et al. CMyc-mediated activation of serine biosynthesis pathway is critical for cancer progression under nutrient deprivation conditions. *Cell Res.* 2015; 25:429–44. [PubMed: 25793315]
12. Maddocks ODK, Berkers CR, Mason SM, Zheng L, Blyth K, Gottlieb E, et al. Serine starvation induces stress and p53-dependent metabolic remodelling in cancer cells. *Nature.* 2013; 493:542–6. [PubMed: 23242140]
13. Maddocks ODK, Athineos D, Cheung EC, Lee P, Zhang T, van den Broek NJF, et al. Modulating the therapeutic response of tumours to dietary serine and glycine starvation. *Nature.* 2017; 544:372–6. [PubMed: 28425994]
14. Kampen KR, Fancello L, Girardi T, Rinaldi G, Planque M, Sulima SO, et al. Translatome analysis reveals altered serine and glycine metabolism in T-cell acute lymphoblastic leukemia cells. *Nat Commun.* 2019; 10:2542. [PubMed: 31186416]
15. Ben-Sahra I, Hoxhaj G, Ricoult SJH, Asara JM, Manning BD. mTORC1 induces purine synthesis through control of the mitochondrial tetrahydrofolate cycle. *Science.* 2016; 351:728–33. [PubMed: 26912861]
16. Pikman Y, Ocasio-martinez N, Alexe G, Kitara S, Diehl FF, Robichaud AL, et al. Targeting serine hydroxymethyltransferases 1 and 2 for T-cell acute lymphoblastic leukemia therapy. *BioRxiv.* 2020
17. Ducker GS, Ghergurovich JM, Mainolfi N, Suri V, Jeong SK, Li SHJ, et al. Human SHMT inhibitors reveal defective glycine import as a targetable metabolic vulnerability of diffuse large B-cell lymphoma. *Proc Natl Acad Sci.* 2017; 114:11404–9. [PubMed: 29073064]
18. García-Cañaveras JC, Lanco O, Ducker GS, Ghergurovich JM, Xu X, da Silva-Diz V, et al. SHMT inhibition is effective and synergizes with methotrexate in T-cell acute lymphoblastic leukemia. *Leukemia.* 2020
19. Melnick JG, Yurkerwich K, Buccella D, Sattler W, Parkin G. Molecular Structures of Thimerosal (Merthiolate) and Other Arylthiolate Mercury Alkyl Compounds. *Inorg Chem.* 2008; 47:6421–6. [PubMed: 18533648]
20. Christen S, Lorendeau D, Schmieder R, Broekaert D, Metzger K, Veys K, et al. Breast Cancer-Derived Lung Metastases Show Increased Pyruvate Carboxylase-Dependent Anaplerosis. *Cell Rep.* 2016; 17:837–48. [PubMed: 27732858]
21. Lorendeau D, Rinaldi G, Boon R, Spincemaille P, Metzger K, Jäger C, et al. Dual loss of succinate dehydrogenase (SDH) and complex I activity is necessary to recapitulate the metabolic phenotype of SDH mutant tumors. *Metab Eng.* 2017; 43:187–97. [PubMed: 27847310]
22. Jones G, Willet P, Glen RC, Leach AR, Taylor R. Development and validation of a genetic algorithm for flexible docking. *J Mol Biol.* 1997; 267:727–48. [PubMed: 9126849]
23. Wishart DS, Knox C, Guo AC, Shrivastava S, Hassanali M, Stothard P, et al. DrugBank: a comprehensive resource for in silico drug discovery and exploration. *Nucleic Acids Res.* 2006; 34:D668–72 [PubMed: 16381955]
24. De Cremer K, Lanckacker E, Cools TL, Bax M, De Brucker K, Cos P, et al. Artemisinins, new miconazole potentiators resulting in increased activity against *Candida albicans* biofilms. *Antimicrob Agents Chemother.* 2015; 59:421–6. [PubMed: 25367916]
25. De Cremer K, De Brucker K, Staes I, Peeters A, Van Den Driessche F, Coenye T, et al. Stimulation of superoxide production increases fungicidal action of miconazole against *Candida albicans* biofilms. *Sci Rep.* 2016; 6:27463 [PubMed: 27272719]
26. Kim SK, Jung WH, Koo JS. Differential expression of enzymes associated with serine/glycine metabolism in different breast cancer subtypes. *PLoS One.* 2014; 9:e101004 [PubMed: 24979213]
27. Delattin N, De Brucker K, Vandamme K, Meert E, Marchand A, Chaltin P, et al. Repurposing as a means to increase the activity of amphotericin B and caspofungin against *Candida albicans* biofilms. *J Antimicrob Chemother.* 2014; 69:1035–44. [PubMed: 24284780]

28. De Keersmaecker K, Atak ZK, Li N, Vicente C, Patchett S, Girardi T, et al. Exome sequencing identifies mutation in CNOT3 and ribosomal genes RPL5 and RPL10 in T-cell acute lymphoblastic leukemia. *Nat Genet.* 2013; 45:186–91. [PubMed: 23263491]
29. Giardina G, Brunotti P, Fiascarelli A, Cicalini A, Costa MGS, Buckle AM, et al. How pyridoxal 5'-phosphate differentially regulates human cytosolic and mitochondrial serine hydroxymethyltransferase oligomeric state. *FEBS J.* 2015; 282:1225–41. [PubMed: 25619277]
30. Witschel M, Stelzer F, Hutzler J, Qu T, Mietzner T, Kreuz K, et al. PYRAZOLOPYRANS HAVING HERBICIDAL AND PHARMACEUTICAL PROPERTIES. US Patent. 2013 WO2013182472A1
31. Ducker GS, Chen L, Morscher RJ, Ghergurovich JM, Esposito M, Teng X, et al. Reversal of Cytosolic One-Carbon Flux Compensates for Loss of the Mitochondrial Folate Pathway. *Cell Metab.* 2016; 23:1140–53. [PubMed: 27211901]
32. Gao X, Lee K, Reid MA, Sanderson SM, Qiu C, Li S, et al. Serine Availability Influences Mitochondrial Dynamics and Function through Lipid Metabolism. *Cell Rep.* 2018; 22:3507–20. [PubMed: 29590619]
33. Bao XR, Ong SE, Goldberger O, Peng J, Sharma R, Thompson DA, et al. Mitochondrial dysfunction remodels one-carbon metabolism in human cells. *Elife.* 2016; 5:e10575 [PubMed: 27307216]
34. Subedi A, Muroi M, Futamura Y, Kawamura T, Aono H, Nishi M, et al. A novel inhibitor of tumorspheres reveals the activation of the serine biosynthetic pathway upon mitochondrial inhibition. *FEBS Lett.* 2019; 593:763–76. [PubMed: 30874300]
35. Ashton TM, Gillies McKenna W, Kunz-Schughart LA, Higgins GS. Oxidative phosphorylation as an emerging target in cancer therapy. *Clin Cancer Res.* 2018; 24:2482–90. [PubMed: 29420223]
36. Zhao X, Guo X, Yue W, Wang J, Yang J, Chen J. Artemether suppresses cell proliferation and induces apoptosis in diffuse large B cell lymphoma cells. *Exp Ther Med.* 2017; 14:4083–90. [PubMed: 29104626]
37. Ho WE, Peh HY, Chan TK, Wong WSF. Artemisinins: pharmacological actions beyond anti-malarial. *Pharmacol Ther.* 2014; 142:126–39. [PubMed: 24316259]
38. Grahame Hardie D. Regulation of AMP-activated protein kinase by natural and synthetic activators. *Acta Pharm Sin B.* 2016; 6:1–19. [PubMed: 26904394]
39. Brown LM. Thimerosal induces apoptosis and G2/M phase arrest in human leukemia cells. *Mol Carcinog.* 2006; 45:694–700. [PubMed: 16739124]
40. Zogg CK. Phosphoglycerate dehydrogenase: potential therapeutic target and putative metabolic oncogene. *J Oncol.* 2014; 2014:524101 [PubMed: 25574168]
41. Fan TWM, Bruntz RC, Yang Y, Song H, Chernyavskaya Y, Deng P, et al. De novo synthesis of serine and glycine fuels purine nucleotide biosynthesis in human lung cancer tissues. *J Biol Chem.* 2019; 294:13464–77. [PubMed: 31337706]
42. Gwynne WD, Hallett RM, Girgis-gabardo A, Bojovic B, Dvorkin-gheva A, Aarts C, et al. Serotonergic system antagonists target breast tumor initiating cells and synergize with chemotherapy to shrink human breast tumor xenografts. *Oncotarget.* 2017; 8:32101–16. [PubMed: 28404880]
43. Hallett RM, Girgis-gabardo A, Gwynne WD, Giacomelli AO, Bisson JNP, Jensen JE, et al. Serotonin transporter antagonists target tumor-initiating cells in a transgenic mouse model of breast cancer. *Oncotarget.* 2016; 7:53137–51. [PubMed: 27447971]
44. Jiang X, Lu W, Shen X, Wang Q, Lv J, Liu M, et al. Repurposing sertraline sensitizes non-small cell lung cancer cells to erlotinib by inducing autophagy. *JCI insight.* 2018; 3:e98921
45. Zhang X, Bai W. Repression of phosphoglycerate dehydrogenase sensitizes triple - negative breast cancer to doxorubicin. *Cancer Chemother Pharmacol.* 2016; 78:655–9. [PubMed: 27473325]
46. Ross KC, Andrews AJ, Marion CD, Yen TJ, Bhattacharjee V. Identification of the serine biosynthesis pathway as a critical component of BRAF inhibitor resistance of melanoma, pancreatic, and non-small cell lung cancer cells. *Mol Cancer Ther.* 2017; 16:1596–609. [PubMed: 28500236]

47. Yoshino H, Nohata N, Miyamoto K, Yonemori M, Sakaguchi T, Sugita S, et al. PHGDH as a key enzyme for serine biosynthesis in HIF2 α - targeting therapy for renal cell carcinoma. *Cancer Res.* 2017; 77:6321–9. [PubMed: 28951458]
48. Devane CL, Liston HL, Markowitz JS. Clinical Pharmacokinetics of Sertraline. *Clin Pharmacokinet.* 2002; 41:1247–66. [PubMed: 12452737]
49. Walpole SC, Prieto-merino D, Edwards P, Cleland J, Stevens G, Roberts I. The weight of nations : an estimation of adult human biomass. *BMC Public Health.* 2012; 12:439. [PubMed: 22709383]
50. Humpton TJ, Hock AK, Maddocks ODK, Vousden KH. p53-mediated adaptation to serine starvation is retained by a common tumour-derived mutant. *Cancer Metab.* 2018; 6:18. [PubMed: 30524726]

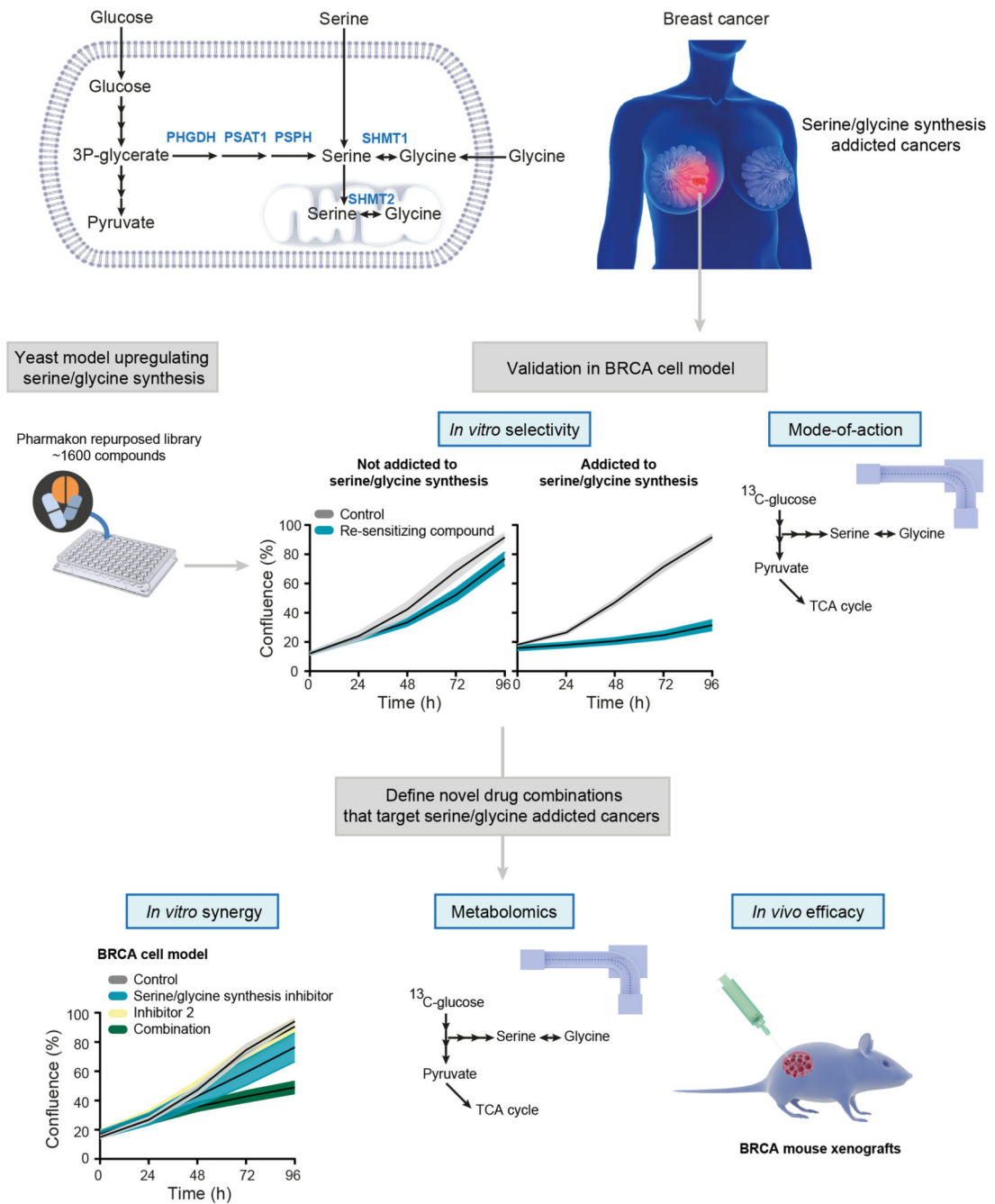


Figure 1. Schematic overview of study design.

In terms of serine/glycine metabolism, breast cancers (BRCA) can largely be divided into serine/glycine uptake or synthesis addicted. Using a yeast model system that upregulates serine/glycine synthesis, we selected repurposed compounds that target serine/glycine synthesis in the breast cancer context. After thorough *in vitro* validation, the most promising, and clinically used, repurposed compound was selected for the rational design of a novel combination therapy for serine/glycine synthesis addicted breast cancer. Human enzymes involved in serine/glycine synthesis are indicated in blue. PHGDH: phosphoglycerate

dehydrogenase; PSAT1: phosphoserine aminotransferase; PSPH: phosphoserine phosphatase; SHMT1/2: cytosolic/mitochondrial serine hydroxymethyltransferase; TCA: tricarboxylic acid.

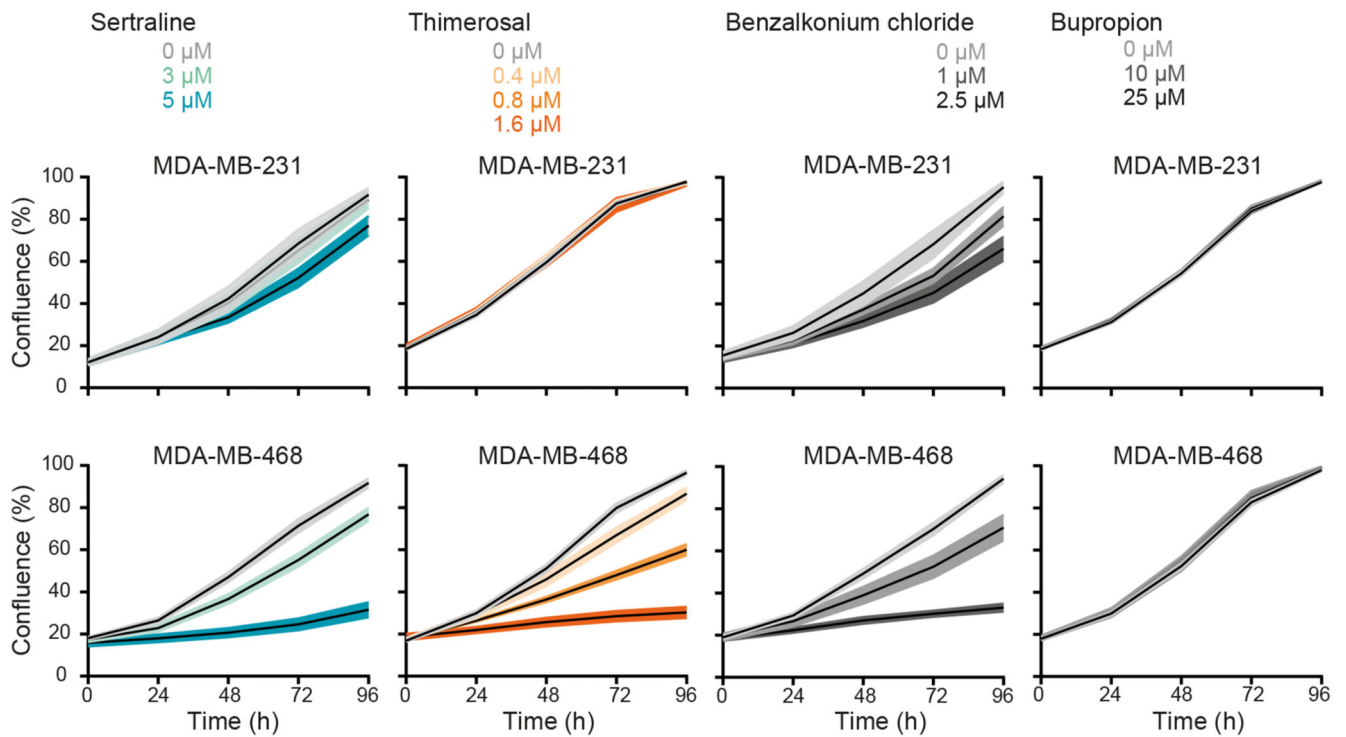


Figure 2. A subset of “re-sensitizing” agents impairs proliferation of serine/glycine synthesis addicted breast cancer cell lines.

Proliferation during 96 hours, as determined by real-time monitoring of cell confluence (%), of MDA-MB-231 (upper) and MDA-MB-468 (lower) cells upon treatment with indicated concentrations of sertraline, thimerosal, benzalkonium chloride and bupropion (left to right). One representative result of three biological replicates, containing each at least three technical replicates, is shown (mean \pm SD).

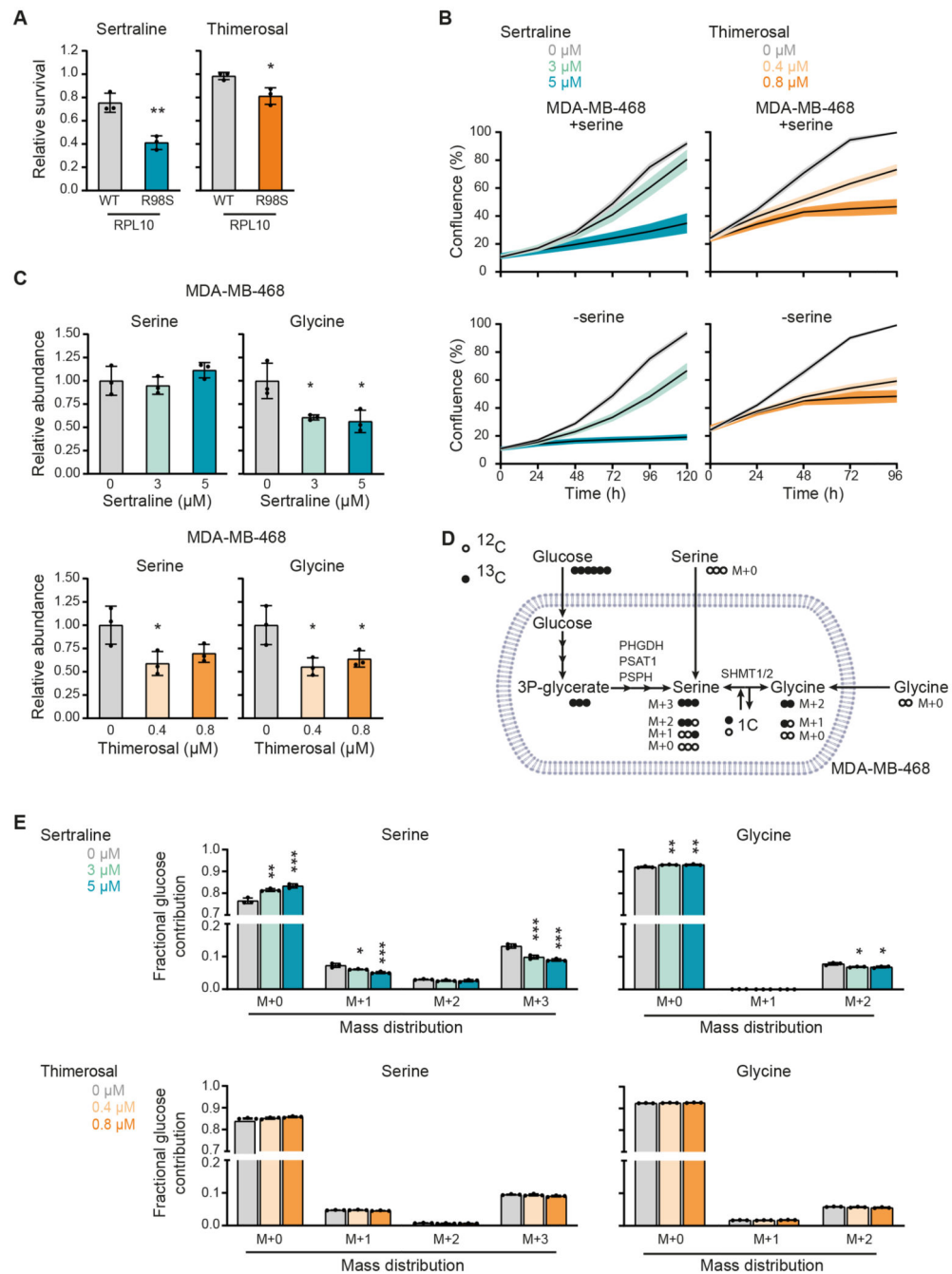


Figure 3. Sertraline and thimerosal target serine/glycine synthesis.

(A) Survival, by measuring cell viability using flow cytometry, of Ba/F3 cells, that express either RPL10 WT or RPL10 R98S, upon treatment with 7.3 μ M sertraline (left) or 1 μ M thimerosal (right) for 48 hours. Values are presented relative to the control treatment (n = 3 individual CRISPR/Cas9 clones with at least two technical replicates in each experiment, Student's t-test). (B) Proliferation, as determined by real-time monitoring of cell confluence (%), of MDA-MB-468 cells cultured in DMEM with (upper) or without (lower) serine (400 μ M) and treated with indicated concentrations of sertraline (left) or thimerosal (right). One

representative result of three biological replicates, containing each at least three technical replicates, is shown. **(C)** Relative abundance of intracellular serine and glycine in MDA-MB-468 cells treated with indicated concentrations of sertraline (upper) and thimerosal (lower) for 72 and 24 hours, respectively (n = 3, One-way ANOVA, Dunnett's multiple comparisons test). **(D)** Schematic representation of carbon incorporation from $^{13}\text{C}_6$ -glucose into serine and glycine. Glucose-derived serine and glycine shows mass shifts of 3 and 2 units (M+3 serine and M+2 glycine), respectively. Cellular uptake of serine and glycine from the cell culture medium will result in unlabeled (M+0) serine and glycine, whereas interconversion between serine and glycine, catalyzed by SHMT1/2, will result in partially labeled serine (M+1 and M+2) and glycine (M+1). **(E)** Serine and glycine mass distribution showing the fractional glucose contribution of each mass upon treatment of MDA-MB-468 cells with indicated concentrations of sertraline (upper) and thimerosal (lower) (n = 3, One-way ANOVA, Dunnett's multiple comparisons). In **(A-C and E)** data are presented as mean \pm SD. *p < 0.05, **p < 0.01, ***p < 0.001.

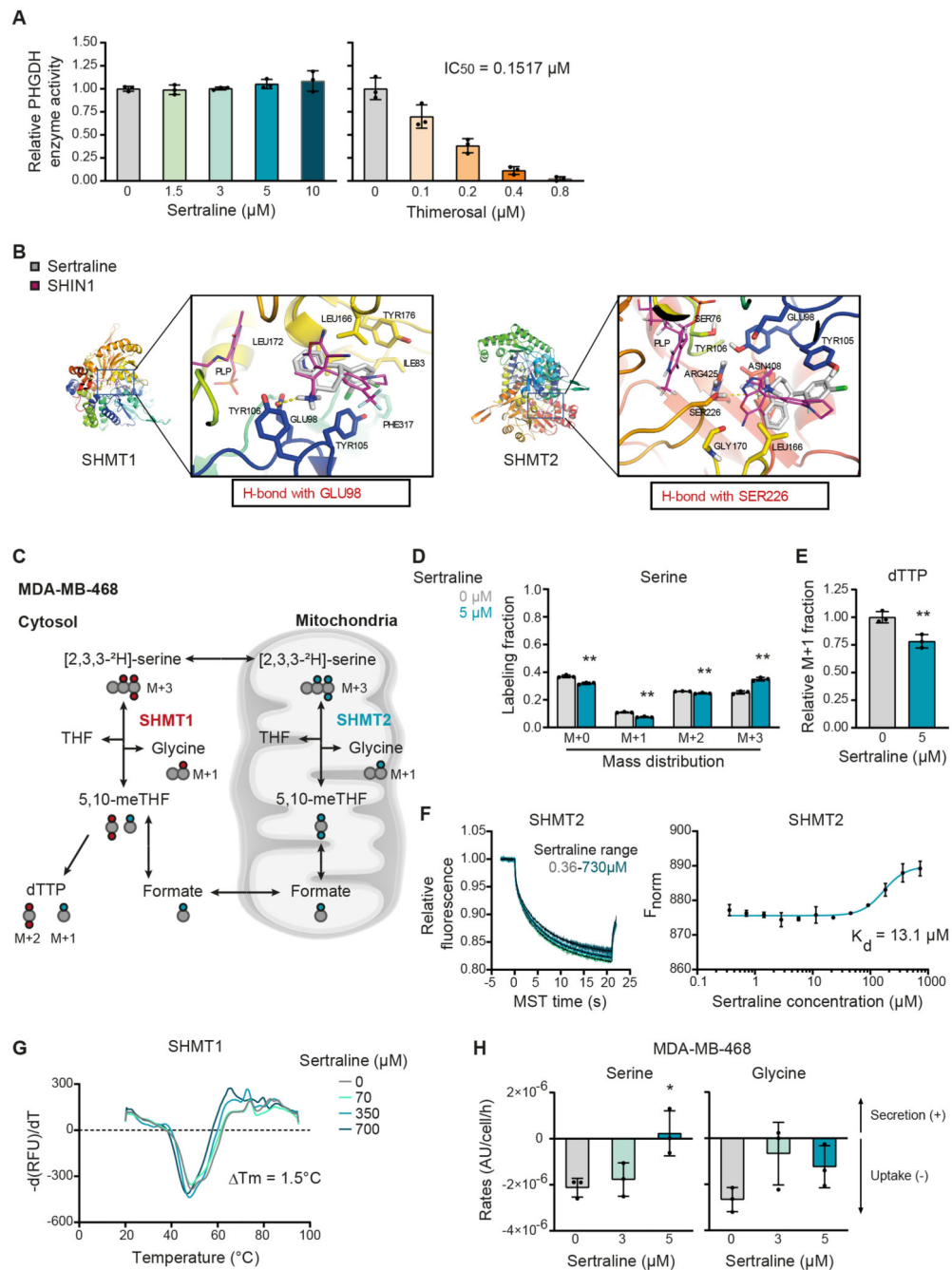


Figure 4. Thimerosal reduces PHGDH activity, while sertraline inhibits SHMT1/2.

(A) PHGDH enzymatic *in vitro* assay, measuring PHGDH activity upon addition of indicated concentrations of sertraline (left) and thimerosal (right). Values are presented relative to the control ($n = 3$). (B) SHMT1 (left) and SHMT2 (right) in complex with sertraline (grey), with a magnified view of the binding pocket showing the interactions formed by sertraline. H-bonds formed by sertraline are presented as yellow dashes. The known SHMT inhibitor SHIN1, with a pyrazolopyran scaffold, is shown in magenta. (C) Schematic overview of isotopic tracing with [2,3,3- ^2H]-serine, showing ^2H incorporation in

downstream metabolites glycine and thymidine (dTTP). Cells taking up fully deuterated (M+3) serine use this to synthesize glycine with one deuterium label (M+1). While cytosolic methylene-THF production, by SHMT1, results in double ^2H -labeled (M+2) dTTP (red dots), mitochondrial SHMT2 will generate single ^2H -labeled (M+1) dTTP (blue dots). **(D)** Serine mass distribution showing the labeling fraction of each mass upon treatment of MDA-MB-468 cells with control (DMSO) or sertraline (5 μM) for 48 hours (n = 3, Multiple t-test). **(E)** Deuterium M+1 labeled dTTP fraction in MDA-MB-468 cells treated with control (DMSO) or sertraline (5 μM) for 48 hours. Values are presented relative to the control (n = 3, Student's t-test). **(F)** Fluorescence distribution curves (left) and dose response curve (right) for SHMT2 incubated with different concentrations of sertraline (0.36 μM - 730 μM). $K_d = 13.1 \mu\text{M}$. Error bars represent the standard deviation of the measurements of two independent repeats. **(G)** Melting temperature (T_m) curves demonstrating sertraline-induced destabilization of SHMT1. One representative result of two biological replicates is shown. **(H)** Serine and glycine uptake (-) and secretion (+) rates (AU/cell/h) of MDA-MB-468 cells treated with indicated concentrations of sertraline for 72 h (n = 3, One-way ANOVA, Dunnett's multiple comparisons). In **(A, D-F and H)** data are presented as mean \pm SD. *p < 0.05, **p < 0.01.

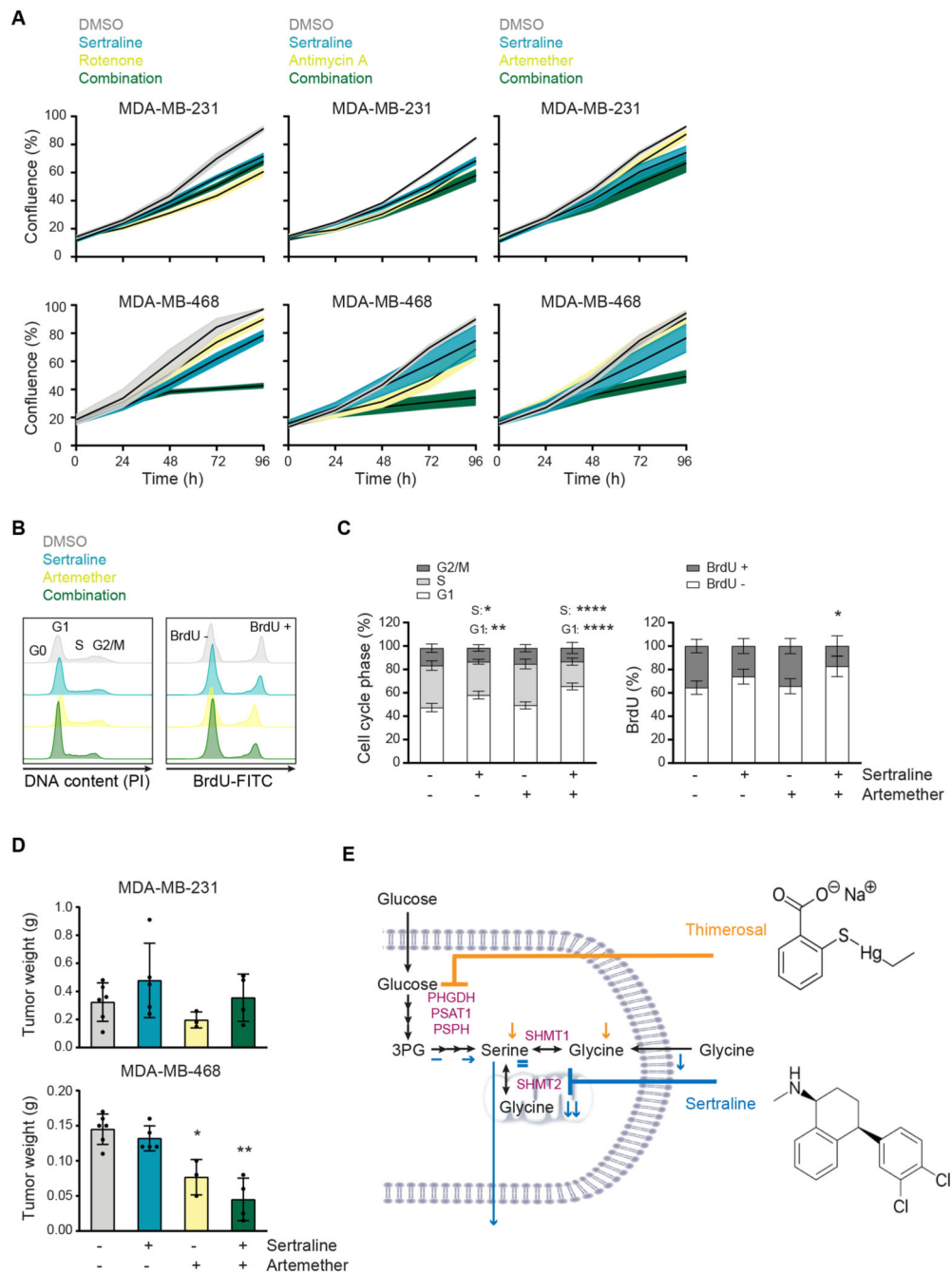


Figure 5. Sertraline has clinical potential, especially in combination with mitochondrial inhibitors.

(A) Proliferation during 96 hours, as determined by real-time monitoring of cell confluence (%), of MDA-MB-231 (upper) and MDA-MB-468 (lower) cells upon treatment with sertraline (5 μ M) in combination with rotenone (50 nM), antimycin A (50 nM) or artemether (80 μ M). One representative result of three biological replicates, containing each at least three technical replicates, is shown. (B) Histograms showing PI cell cycle analysis (left) and BrdU incorporation (right) of MDA-MB-468 cells treated with DMSO, sertraline (5 μ M)

and/or artemether (80 μ M) for 24 hours. One representative result of three biological replicates is shown. **(C)** Quantification of **(B)** pooling all three biological replicates (n = 3, Two-way ANOVA, Dunnett's multiple comparisons test). **(D)** Tumor weight (g) of MDA-MB-231 (left flank) and MDA-MB-468 (right flank) mouse xenografts after treatment with DMSO, sertraline (2.5 mg/kg), artemether (40 mg/kg) or a combination of both compounds for 4 weeks (n = 3, Kruskal-Wallis test, followed by Mann-Whitney U test). **(E)** Schematic overview of the mode-of-action of sertraline and thimerosal. In **(A, C and D)** data are presented as mean \pm SD. *p < 0.05, **p < 0.01, ****p < 0.0001.

Table 1
Computational docking of sertraline to SHMT1 and SHMT2.

Docking scores for sertraline into the active pocket of SHMT1 and SHMT2. The already identified dual SHMT1/2 inhibitor SHIN1, based on a pyrazolopyran scaffold, was used as reference structure.

Interaction	Docking score
SHMT1_sertraline1 ^a	61.49
SHMT1_sertraline2 ^a	59.68
SHMT1_SHIN1	66.65
SHMT2_sertraline	51.34
SHMT2_SHIN1	65.39

^a 1 and 2 refer to the two conformations in which sertraline can bind to SHMT1.